Individual and combined effects of diuron and light reduction on marine microalgae

King, O. C., van de Merwe, J. P., Brown, C. J., Warne, M. S. J. & Smith, R. A

Original citation:
King, OC, van de Merwe, JP, Brown, CJ, Warne, MSJ & Smith, RA 2022, 'Individual and combined effects of diuron and light reduction on marine microalgae', Ecotoxicology and Environmental Safety, vol. 241, 113729.
https://doi.org/10.1016/j.ecoenv.2022.113729

DOI 10.1016/j.ecoenv.2022.113729
ISSN 0147-6513

Publisher: Elsevier

Ecotoxicology and Environmental Safety 241 (2022) 113729

Contents lists available at ScienceDirect

Ecotoxicology and Environmental Safety

journal homepage: www.elsevier.com/locate/ecoenv

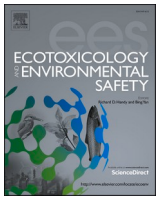

Individual and combined effects of diuron and light reduction on marine microalgae

Olivia C. King [a,*], Jason P. van de Merwe [a], Christopher J. Brown [a], Michael St. J. Warne [b,c,d], Rachael A. Smith [e]

[a] Coastal and Marine Research Centre, Australian Rivers Institute, School of Environment and Science, Griffith University, Gold Coast, Queensland 4222, Australia
[b] School of Earth and Environmental Sciences, University of Queensland, Brisbane, Queensland 4067, Australia
[c] Water Quality and Investigations, Queensland Department of Environment and Science, Brisbane, Queensland 4102, Australia
[d] Centre for Agroecology, Water and Resilience, Coventry University, West Midlands CV1 5FB, UK
[e] Office of the Great Barrier Reef, Department of Environment and Science, Queensland Government, Brisbane, Queensland 4000, Australia

ARTICLE INFO

Edited by Dr. Hyo-Bang Moon

Keywords:
Multiple stressors
Coastal ecosystems
Microalgae
Phytotoxicity
Photosystem II herbicides
Light availability

ABSTRACT

Coastal ecosystems such as those in the Great Barrier Reef (GBR) lagoon, are exposed to stressors in flood plumes including low light (caused by increased turbidity) and agricultural pesticides. Photosystem II (PSII)-inhibiting herbicides are the most frequently detected pesticides in the GBR lagoon, but it is not clear how their toxicity to phototrophic species depends on light availability. This study investigated the individual and combined effects of PSII-inhibiting herbicide, diuron, and reduced light intensity (as a proxy for increased turbidity) on the marine diatom, *Phaeodactylum tricornutum*. Effective quantum yield (EQY) and cell density were measured to calculate responses relative to the controls over 72-h, in tests with varying stressor intensities. Individually, diuron concentrations (0.1–3 μg l^{-1}) were not high enough to significantly reduce growth (cell density), but led to decreased EQY; while, low light generally led to increased EQY, but only reduced growth at the lowest tested light intensity (5 μmol photons m^{-2} s^{-1}) after 48-hours. *P. tricornutum* was less affected by diuron when combined with low light scenarios, with increased EQY (up to 163% of the controls) that was likely due to increased electron transport per photon, despite lesser available photons at this low light intensity. In contrast, growth was completely inhibited relative to the controls when algae were simultaneously exposed to the highest stressor levels (3 μg l^{-1} diuron and 5 μmol photons m^{-2} s^{-1}). This study highlights the importance of measuring more than one biological response variable to capture the combined effects of multiple stressors. Management of water quality stressors should consider combined impacts rather than just the impacts of individual stressors alone. Reducing suspended sediment and diuron concentrations in marine waters can decrease harmful effects and bring synergistic benefits to water quality.

1. Introduction

Second to climate change, degraded water quality from human activities and land-use changes have been identified as the greatest risk to marine and coastal ecosystems, globally (Waterhouse et al., 2017; Smale et al., 2019). Inshore areas are often exposed to the highest frequency and concentrations of water quality stressors such as nutrients, sediments and pesticides, which are transported via flood plumes following elevated rainfall (Devlin et al., 2012; Waterhouse et al., 2021). Reducing anthropogenic inputs such as total suspended sediments (TSS) and agricultural pesticides are two of the four water quality targets to help build resilience of Great Barrier Reef (GBR) ecosystems (Australian Government and Queensland Governments, 2018).

Assessing the combined effects of more than one stressor is a high priority for environmental management (Van den Brink et al., 2016; Waterhouse et al., 2017); however, the ability to consider multiple stressors is limited as empirical data are often lacking (Crain et al., 2008; Brown et al., 2014; Chariton et al., 2016; Côté et al., 2016). As a consequence, ecological risk assessments (ERAs) which are frequently used to inform management decisions still consider stressor impacts separately (Brodie et al., 2013; Waterhouse et al., 2017), despite the fact that stressors co-occur (Waterhouse et al., 2017; Negri et al., 2020;

* Corresponding author.
E-mail address: olivia.king@griffithuni.edu.au (O.C. King).

https://doi.org/10.1016/j.ecoenv.2022.113729
Received 15 March 2022; Received in revised form 26 May 2022; Accepted 30 May 2022
Available online 3 June 2022

Warne et al., 2020b), meaning that combined or interacting effects are not often considered or assessed by management bodies.

Increased turbidity, due to elevated TSS and increased phytoplankton biomass (resulting from eutrophication), cause a decrease in the amount of photosynthetically active radiation (PAR) available to aquatic photosynthetic organisms such as seagrasses, macroalgae and microalgae (Devlin et al., 2012; Fabricius et al., 2014). Photosystem II (PSII)-inhibiting herbicides are amongst the most common pesticides detected year-round in the waterways that discharge to the GBR (Spilsbury et al., 2020; Warne et al., 2020b), and in the GBR lagoon itself, Australia (Thai et al., 2020). Due to their mode of action, these herbicides specifically target phototrophic organisms. They exert their toxicity by blocking electron transport that is required for growth and survival (Ahrens, 1994), and by increasing intracellular concentrations of reactive oxygen species (ROS), which can cause irreversible cell damage (Chen et al., 2012). Reduced light, in combination with PSII-inhibiting herbicides can also significantly affect physiological responses that directly and indirectly impact phototrophic growth, abundance and the distribution of primary producers (Lee et al., 2007; King et al., 2021).

Marine microalgae are important primary producers that form the base of many food-webs and contribute to nutrient cycling in marine waters (Arrigo, 2005; Reynolds et al., 2014). In the GBR lagoon, marine microalgae communities are dominated by small flagellates and pennate diatoms (Bell and Elmetri, 1995). Diatoms are useful biological indicators as they rapidly respond to changing water quality conditions that allow a better understanding of the health and resilience of aquatic ecosystems (Armbrust, 2009). Marine diatoms are sensitive to light, nutrients and agrochemicals such as PSII-inhibiting herbicides (Armbrust, 2009; Magnusson et al., 2010; Thomas et al., 2020). Thus, identifying their phytotoxic and physiological responses to water quality stressors is important for managing marine ecosystems more broadly.

Photosynthetic measurements, such as chlorophyll-a fluorescence, are often directly associated with energy reserves and growth (Ralph et al., 2007b), and thus act as sensitive indicators to assess stressor responses. For example, exposure to various PSII-inhibiting herbicides reduced the EQY, photosynthetic efficiency and growth rate of tropical microalgae and coral symbionts (Magnusson et al., 2008; Marzonie et al., 2021), demonstrating a strong correlation between reduced photosynthetic measurements and increased toxicity. However, the effects of chronic low light on photosynthetic measurements, such as fluorescence-based estimates, are less defined due to experimental, field-based and scale-related variables (Ralph et al., 2007a). It is evident that PSII-inhibiting herbicides and light availability both affect the photosynthetic apparatus of phototrophs (Gomes and Juneau, 2017) via various individual physiological responses. However, further experimental research is needed to assess the effects of simultaneous exposure to these two stressors (King et al., 2021).

This study aims to assess the phytotoxic and physiological responses of a unicellular marine microalga to environmentally relevant concentrations of a PSII-inhibiting herbicide and reduced light availability. Specifically, we test how the simultaneous acute and chronic exposures of varying concentrations of diuron and light intensity affect the physiological responses of marine diatom, *Phaeodactylum tricornutum*. Individual and combined effects on effective quantum yield (chlorophyll-a fluorescence) and growth rate (cell density) were measured over a 72-hour exposure period.

2. Methods

2.1. Microalgae isolation and culture maintenance

The test organism *P. tricornutum* is a marine pennate diatom that is widely distributed in estuarine and coastal areas (ISO, 2016), and is considered to be an excellent model species for assessing physiological and biological endpoints (Bengtson Nash et al., 2005; Schreiber et al., 2007). *P. tricornutum* (CSIRO strain CS-29) was purchased as a stock culture from the CSIRO Australian National Algal Culture Collection (ANACC, Tasmania, Australia), and cultured under axenic conditions in 50 ml Erlenmeyer flasks. The growth medium was sterile seawater supplemented with f/2 nutrients and silicate (ANACC, Tasmania, Australia). Cultures were maintained at 20 °C in an incubator, following batch culturing methods (ISO, 2016), which included growth medium without aeration, continuous illumination (80 μmol photons m^{-2} s^{-1}) from cool white fluorescence tubes (Sylvania Grolux, Germany) and shaking at 90 RPM. Culture maintenance conditions are the same as those used at the CSIRO Australian National Algal Culture Collection service prior to dispatch (i.e., 20 °C, 80 μmol photons m^{-2} s^{-1}), suggesting that the *P. tricornutum* culture would be well acclimated to the control conditions prior to test commencement.

Effective quantum yield (EQY) of the algae suspension was measured before testing to determine photochemical efficiency or 'health' of the culture. Under 80 μmol photons m^{-2} s^{-1}, a steady state EQY of ≥ 0.5 was considered healthy, and that the culture was suitable for testing (Ralph and Gademann, 2005).

2.2. Toxicant preparation

Diuron (CASRN 330-54-1; analytical standard, > 95% purity) and methanol (HPLC-grade 99.9%) were obtained from Sigma Aldrich, New South Wales, Australia. In sterilised glassware, stock solutions of diuron were made up in methanol as the carrier solvent. Diuron concentrations were 1:3 serial diluted (3, 1, 0.3 and 0.1 μg l^{-1}) from freshly made stock solutions immediately prior to each test. Solvent (methanol) controls (at 0.08%; held identical for each treatment) were included in each test.

It is recommended that exposure concentrations are measured for compounds with a log $K_{ow} > 3$ (Riedl and Altenburger, 2007). As diuron is non-volatile, water soluble (37.4 mg l^{-1} at 25 °C; BCPC, 2012) and has a low octanol-water coefficient (log K_{ow} of 2.85 at 25 °C; BCPC, 2012), adsorption or binding to test vessels is unlikely (BCPC, 2012). On this basis, nominal concentrations of diuron were deemed accurate for the chosen exposure regimes.

2.3. Microalgae growth and calibration curve

P. tricornutum axenic cultures showed a ~60-h lag-phase before entering exponential growth phase. Therefore, all algae used in the tests were sub-cultured 72-hours prior to test initiation to ensure cultures were in the exponential growth phase at test initiation.

A calibration curve between optical density and cell density was established by measuring the optical density by spectrophotometric absorbance (at 685 nm (OD_{685})) and counting the number of cells ($\times 10^4$) with a haemocytometer (Neubauer, Germany). This was done in three 72-h old cultures and growth media blanks that were 1:2 serially diluted ten times. A relationship between absorbance and cell density was established using a linear regression curve as per Eq. 1:

$$\text{Cell density } (y) = 4179{\cdot}6 \times (\textit{absorbance at 685 nm}) - 172{\cdot}5 \ (R^2 = 0.99) \quad [1]$$

2.4. Range-finding for diuron and decreased light exposure

Range finding toxicity tests were conducted to identify concentrations of each stressor that were likely to cause a 0–90% effect on a sensitive endpoint (USEPA, 2012). For diuron, these concentrations were 0.4, 0.8, 1.6, 3.1, 6.3, 12.5, 25 and 50 μg l^{-1}, which caused an 8–94% inhibitory EQY after a 2-h exposure period. For light, a decreasing gradient ranging from optimal light to complete darkness (80, 55, 35, 20, 5, >0.01 μmol photons m^{-2} s^{-1}) inhibited growth (15–100%) after a 96-hour exposure period.

Phototrophic species will often acclimate to changes in light before

growth is negatively affected at later exposure times (Dubinsky and Stambler, 2009); therefore, the range finding test for decreased light was conducted over a longer exposure period. In comparison, diuron can inhibit the sensitive endpoint, photosynthesis, almost immediately due to the direct impairment of photosystem II (Morin et al., 2018); therefore, a 2-hour exposure was sufficient.

The concentration/level of stressor at which an ~50% effect occurred was set as the highest exposure threshold, to allow for increased effect when combined with the other stressor. Definitive exposure concentrations/levels were as follows; diuron at 0.1, 0.3, 1 and 3 μg l^{-1} and decreased light at 80, 20 and < 5 μmol photons m^{-2} s^{-1}. The lower diuron concentrations were within the lower to mid-range of maximum concentrations detected in the GBR lagoon (i.e., 0.8 μg l^{-1} in 2017–18 (Gallen et al., 2019)), and the higher concentrations were included to represent potential future increases in diuron concentrations in the GBR lagoon. The range-finding tests for light indicated that responses between 80 and 20 μmol photons m^{-2} s^{-1} were similar, so including additional light levels between these would not provide meaningful information.

All experiments were performed on four separate occasions (called 'blocks'), using independent algae cultures. Within each block, two replicates of algae-only control flasks were initially included at each light level to investigate variability. This resulted in low standard deviation (relative to the mean) values of < 5% (EQY) and < 10% (growth rate) over the 72-hour exposure period. The only exception to this was for growth rate at 72-hours under 20 μmol photons m^{-2} s^{-1} where variation reached 19%. As space within the incubator was limited, the number of control flasks in subsequent blocks was therefore reduced to one, to prioritise a greater number of treatment levels. This gradient design is optimal for detecting non-linear effects of stressors (Kreyling et al., 2018).

2.5. Toxicity tests

Exposures were conducted in 50 ml Erlenmeyer glass flasks. Each flask contained 20 ml of growth medium and algae cells at a starting cell density of 1×10^4 cells ml^{-1}, determined using hemocytometer counts. Flasks were covered with permeable film (PARAFILM® sealing tape, Sigma Aldrich) to permit gas exchange, but minimise evaporation. Cultures were incubated following standard culture maintenance conditions (see Section 2.1) for 72-hours prior to test initiation, to ensure cultures were in the exponential growth phase at test initiation.

Four blocks were tested to calculate the EQY and growth rate of *P. tricornutum* to diuron exposure and light reduction. Each test and control treatment were run once within each block, allowing the four blocks to act as four replicates. A total of 18 flasks were used per block, containing four diuron treatments (0.1, 0.3, 1 and 3 μg l^{-1}) plus a solvent (methanol) control (at 0.08%) and an algae control, each at three light levels of 5, 20 and 80 μmol photons m^{-2} s^{-1} (n = 72). Flasks were wrapped in foil to achieve two levels of reduced light coverage (from optimal of 80 μmol photons m^{-2} s^{-1}). Thus, each block contained treatments of diuron and light, both alone and in combination (Supplementary material, Table S1).

Measurements of chlorophyll-a fluorescence (effective quantum yield, EQY) were recorded at 0-hours (immediately before dosing), 2, 24, 48 and 72-h after dosing while measurements of absorbance (as a proxy for cell density and growth) were recorded at 0, 24, 48 and 72-h after dosing to cover acute and chronic exposures.

The water quality parameters of the test flasks throughout the exposure tests were salinity 33.5‰, temperature 20 ± 2 °C and pH of 8 ± 0.2.

2.5.1. Measurements of effective quantum yield

EQY (or photosynthetic efficiency of PSII) was determined via measures of variable chlorophyll-a fluorescence, which was quantified by measuring the amount of light re-emitted at longer wavelengths than the defined wavelength that the microalgae were exposed to (Maxwell and Johnson, 2000). Two sub-sample aliquots (300 μl) of blanks (media only), controls and exposed algae from each test vessel were transferred into clear 96-well microplates (Greiner Bio-One, Austria) and immediately placed in the Maxi-Imaging-PAM (Maxi-iPAM Chlorophyll Fluorometer M-Series, Heinz Walz GmbH, Germany) to record chlorophyll-a fluorescence response (Schreiber et al., 2007). To activate and record chlorophyll-a fluorescence, three light intensities were emitted from the iPAM at 450 nm with varying light intensities: a measuring light of 1 μmol photons m^{-2} s^{-1} (= 4) and modulation frequency of 8 Hz, an actinic light of 11 μmol photons m^{-2} s^{-1} (= 1) for 120 s prior to measurement and a saturating light of 5000 μmol photons m^{-2} s^{-1} applied as six pulses in 30 second intervals. The gain and damping were both set to 2.

The ImagingWinGigE software program (v2.45b; Walz GmbH) was used to obtain maximum (Fm′) and minimum (F) chlorophyll-a fluorescence parameters of each individual well (sample) in the 96-well plate. Actinic light was switched on, followed by a saturating pulse, upon which F and Fm′ were recorded. The recording of Fm′ and F continued every 30 ss until steady-state chlorophyll-a fluorescence was reached (within 2 min). The data of the last five saturating pulse measurements were averaged once steady-state chlorophyll-a fluorescence was reached.

The effective quantum yield (EQY) for each well (sample) was calculated according to Eq. 2:

$$\mathrm{EQY} = \frac{F\mathrm{m}' - F}{F\mathrm{m}'} \quad [2]$$

EQY-values were averaged across the two sub-samples. To correct for any temporal drift in the EQY-values of the controls, the test EQY-values were expressed as a percentage of the control at the same point in time, calculated according to Eq. 3:

$$\mathrm{EQY}\ (\%)\ \text{as a percentage of the } \textit{controls} = \frac{\mathrm{EQY}_{test}}{\mathrm{EQY}_{control}} \times 100 \quad [3]$$

Calculating EQY as a percentage of the controls allowed plotting of stressor response curves, where values less than and greater than 100% indicate inhibition and increased EQY relative to the controls, respectively.

2.5.2. Measurements of growth rate

Cell density was determined via measures of spectrophotometric absorbance at 685 nm (OD_{685}). At each time point, two sub-sample aliquots (100 μl) of blanks, controls and exposed algae from each test flask were transferred into clear 96-well microplates (Greiner Bio-One, Austria) and immediately placed in the Tecan Spark® multimode microplate reader (Tecan, Männedorf, Swizerland) to measure absorbance. All absorbance measurements were converted to cell density using Eq. 1, and the average (cell density) of the two sub-samples (from each flask) was used in the following growth calculations.

The average specific growth rate (μ) for each test (flask) was expressed as the logarithmic change in cell density over time, and was calculated using the time of the test start (t_0), the time of the test termination (t_L), the initial cell density (N_0) and the measured cell density at time t_L (N_L) (Eq. 4).

$$\mu = \left(\frac{\ln N_L - \ln N_0}{t_L - t_0}\right) \quad [4]$$

μ -values were averaged across the two sub-samples. As some test results had greater μ-values than the controls, test values were expressed as a percentage of the control, and calculated using Eq. 5:

$$\text{Growth } \textit{rate}\ (\%)\ \text{as a percentage of the } \textit{controls} = \frac{\mu_{\mathrm{test}}}{\mu_{\mathrm{control}}} \times 100 \quad [5]$$

Calculating growth rate as a percentage of the controls allowed plotting of stressor response curves, where values less than and greater

than 100% indicate inhibition and stimulation relative to the controls, respectively. Negative values were rare, but occurred when growth in the test was negative.

2.6. Statistical analysis

Standard stressor-response curves and column graphs, both with standard error of the mean (SEM) bars, were plotted using a four-parameter sigmoid regression model in GraphPad Prism 8 (version 8.4.3). Two-sample t-tests were used to determine significant differences in column graphs, with the difference considered significant when $p \leq 0.05$.

Effect concentration (ECx) values were determined by non-linear regression of the stressor-response curves using the least squares method within the 'ECanything' function. Diuron concentrations (μg l^{-1}) that affect EQY and growth rate by 10% (EC10) and 20% (EC20) with 95% confidence intervals at each light level were calculated for 2, 24, 48 and 72-h exposures.

Predicted versus observed values were then used to identify expected interaction types between diuron and reduced light. The predicted (or additive) value was calculated using the Independent Action (IA) mathematical model of joint action (Eq. 6) (Bliss, 1939), where R_A and R_B are the individual responses (%) of stressor A and B, respectively.

$$\text{Predicted (additive) value} = 1 - (1 - R_A) \times (1 - R_B) \quad [6]$$

This predictive model is commonly used in ecotoxicology to estimate the environmental impact of multiple stressors that act on different target sites within an organism. The observed value was the measured combined response (%) from the toxicity tests. The expected interaction type (i.e., antagonistic, additive or synergistic) for each treatment combination was calculated by subtracting the predicted (additive) value (%) from the observed value (%). When the observed response was greater than the predicted value (i.e., 150% and 110%, respectively), the algae were doing 'better' than the controls, and therefore an antagonistic interaction occurred. In contrast, when the observed response was less than the predicted value (i.e., 70% and 10%, respectively), the algae were doing 'worse' than the controls and therefore a synergistic interaction occurred. When the observed value was equal to the predicted value, the algae were considered to be no different to the controls and thus were response additive (consistent with Independent Action).

The individual effects of diuron and reduced light with exposure duration, on EQY and growth rate inhibition were tested using linear mixed effects models with the R statistical software package, "lmer". The combined effects of diuron and reduced light on EQY and growth rate were tested by fitting generalised additive mixed models (GAMMs) with the R statistical software package, "mgcv". Significance was set at the 5% level for all tests ($\alpha = 0.05$).

3. Results and discussion

3.1. Validity of the tests

The cell density of all controls increased by at least 16-fold in 72-h (data not shown), and flasks were continuously shaken during the test to minimise variations in pH, successfully meeting the required test validity criteria for algae growth inhibition (ISO, 2016). No internationally recognised standard method was available to test validity conditions for the chlorophyll-a fluorescence endpoint. However, prior to testing ($t = 0$), the EQY of all algae suspension was ≥ 0.5. All control EQY values for each time point are provided in Supplementary Material, Table S2.

The mean coefficient of variation (standard deviation relative to the mean) values of EQY and growth rate responses during the whole test period in replicate control treatments did not exceed 20%, which is within the 35% stipulated by OECD (2011). Similarly, solvent (methanol) controls did not exceed 20% effect (either positively or negatively), except for two growth values where variation reached 76% relative to the controls (i.e., 24% growth inhibition) and 185% relative to the controls (i.e., 85% growth stimulation) at 72-hours under 80 μmol photons m^{-2} s^{-1} and at 48-hours under 5 μmol photons m^{-2} s^{-1}, respectively.

In some instances, the data were deemed to be invalid for inclusion in the analysis. Growth rate data from block 1 (replicate 1) was excluded due to an error with the plate-reader. The 24-h growth rate measurements were highly variable showing both increased and decreased growth rates relative to the controls. This is likely to be due to cell density still being too low at 24-h because higher cell density increases precision, a response lag-phase, stimulated growth as a final mechanism for survival, or biological reasons such as short-term utilisation of the stressor for nutrient purposes.

3.2. Exposure to diuron alone

3.2.1. Effects on effective quantum yield

The four-parameter sigmoidal regression curve demonstrated a typical stressor-response relationships between diuron and EQY (Fig. 1A). There was a significant interaction between diuron and exposure duration on EQY ($\chi^2 = 126.7$, $df = 25$, $p = 1.46 \times 10^{-15}$). Relative to the controls, EQY was most impacted after 2-hours of exposure to 3 μg l^{-1} of diuron with a mean ± SEM of 48 ± 2.1% ($R^2 = 0.97$), compared to 61 ± 3.5% ($R^2 = 0.46$), 67 ± 3.0% ($R^2 = 0.85$) and 68 ± 3.0% ($R^2 = 0.85$) after 24, 48 and 72-h, respectively (Fig. 1A). Reduced EQY at 2-h may indicate a specific effect on the algae, namely PSII-inhibition, or that maximum cellular uptake hadn't yet occurred; while, later readings indicate delayed phytotoxicity, and includes both specific and non-specific effects (Escher et al., 2008).

It was observed that EQY decreased when algae were exposed to increasing diuron concentrations. This study determined 2-h EC_{10} and EC_{20} (EQY, inhibition) values of 0.50 and 0.96 μg l^{-1} diuron, respectively (Table 1). The EC_{10} value fell within the lower range of previously published EC_{10} (photosynthetic efficiency) values for *P. tricornutum* after acute exposures to diuron; 2-h EC_{10} value of 0.80 μg l^{-1} (Muller et al., 2008) and 4-h EC_{10} value of 0.42 μg l^{-1} (Magnusson et al., 2010). There were no available diuron EC_{20} toxicity values available in the literature for *P. tricornutum* exposed to diuron. However, the EC_{20} value determined in this study was less than previously reported acute toxicity values of diuron to *P. tricornutum*: 2-h EC_{50} (photosynthetic efficiency) of 18 μg l^{-1} (Muller et al., 2008), 4-h EC_{50} (photosynthetic efficiency) of 2.7 μg l^{-1} (Magnusson et al., 2010), 4.5-h EC_{50} (photosynthetic efficiency) of 1.8 μg l^{-1} (Sjollema et al., 2014a) and an IC50 (undefined acute exposure, photosynthetic efficiency) of 3.3 μg l^{-1} (Schreiber et al., 2002).

Finally, a decrease in EQY (suggesting improved photosynthetic efficiency) over time was observed for diuron exposed diatoms. This decrease may be attributed to factors such as; low starting densities of the algae (i.e. 1×10^4 cells ml^{-1}, as per the ISO, 2016 methodology), where the decrease in EQY over time might be less visible if using higher starting densities of algae; or, algae recovery may begin to occur over time as the impacts of diuron on EQY occur rapidly. Previous studies have reported faster recovery of chlorophyll fluorescence when marine benthic diatoms are exposed to lower concentrations of diuron over longer time periods (Du et al., 2021). Similarly, the EQY of dinoflagellates recovered to control levels after chronic exposure to their lowest tested concentration of diuron (1 μg l^{-1}) (Howe et al., 2017).

3.2.2. Effects on growth rate

There was no significant interaction between diuron and exposure duration on growth rate ($\chi^2 = 3.938$, $df = 16$, $p = 0.999$). Compared to the controls, growth inhibition was observed for only one test condition, 90 ± 7% (mean ± SEM) observed at 0.11 μg l^{-1} of diuron after 48-h (Fig. 1B). The remaining mean values for the diuron only exposures

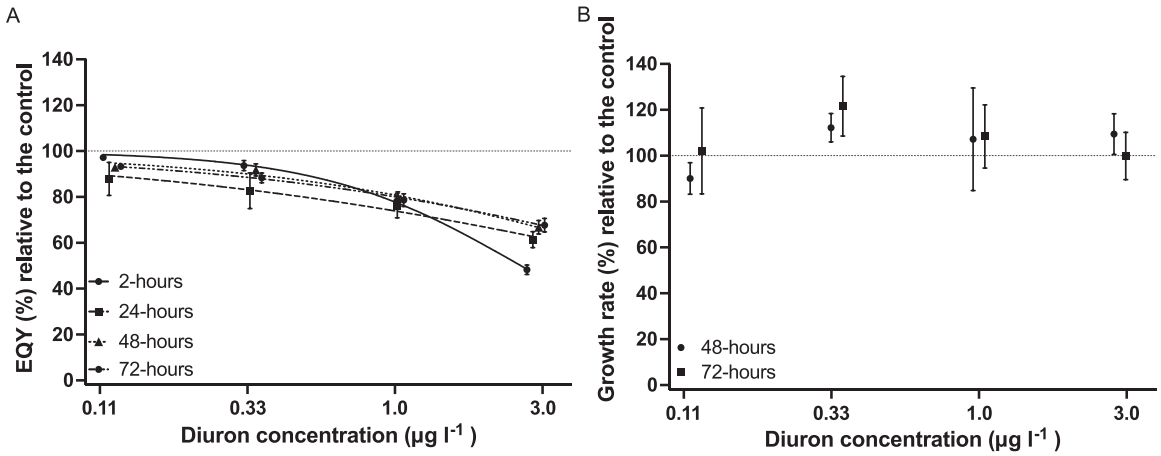

Fig. 1. Stressor response curves of the mean (± SEM) for the effective quantum yield (A; $n = 4$) and growth rate (B; $n = 3$) of *P. tricornutum* expressed as a percentage of the controls, when exposed to a range of diuron concentrations. Responses (%) have been expressed as a percentage of the control (dashed line) so that the controls equal 100%, and values less than and greater than 100% indicate decreased and increased EQY/growth, respectively (e.g., 90% and 120% values on the y-axis are equivalent to 10% reduction of photosynthetic efficiency/growth and 20% increase of photosynthetic efficiency/growth relative to the controls, respectively). Stressor-response curves could not be fitted to the growth rate data ($R^2 = \leq 0.01$ for 48 and 72-hours).

Table 1
EC_x values of diuron concentrations (µg l^{-1}) that decrease EQY and growth rate by 10% (EC_{10}) and 20% (EC_{20}) with 95% confidence intervals in parentheses at each light level (µmol photons m^{-2} s^{-1}) at various exposure times. R^2 values explain the variance around the four-parameter sigmoid regression model fitted values. Growth was not reached for 80 and 20 µmol photons m^{-2} s^{-1} after 48 and 72-h, thus denoted by NR to indicate no relationship as the model could not fit the data. An asterisk indicates the upper and/or lower confidence intervals could not be defined.

Exposure time (hours)		Light level (µmol photons m^{-2} s^{-1})	EC_{10} (95% CI)	EC_{20} (95% CI)	R^2
Effective quantum yield					
Acute	**2**	**80 – control**	0.50 (0.27–0.78)	0.96 (0.62–1.3)	0.97
		20	0.65 (0.44–0.88)	1.1 (0.87–1.4)	0.98
		5	0.62 (0.32–0.98)	1.1 (0.73–1.5)	0.96
	24	**80 – control**	0.50*	1.4 (*–7.0)	0.46
		20	0.16*	0.55 (*–3.0)	0.56
		5	0.72*	1.3*	0.56
Chronic	**48**	**80 – control**	0.46 (2.0×10^{-7}–1.3)	1.3 ($5.4 \times {}^{-3}$–2.4)	0.85
		20	0.36 (2.5×10^{-7}–1.2)	1.1 (2.3×10^{-5}–2.2)	0.82
		5	0.72 (0.15–1.5)	1.4 (0.54–2.1)	0.88
	72	**80 – control**	0.15 (*–1.1)	0.72 (*–2.3)	0.85
		20	0.96 (0.12–1.9)	2.0 (0.62–2.8)	0.85
		5	0.70 (0.05–1.6)	1.5 (0.29–2.3)	0.87
Growth rate					
Chronic	**48**	**80 – control**	NR	NR	0.01
		20	NR	NR	-1.6
		5	0.30 (0.02–1.1)	0.46 (0.07–1.3)	0.62
	72	**80 – control**	NR	NR	-0.13
		20	NR	NR	-0.75
		5	1.6 (0.16–*)	1.8 (0.39–*)	0.55

ranged from 100% to 122% suggesting a slight increase in growth (i.e., > 100%). However, in all but two cases (i.e., 0.11 µg l^{-1} and 3 µg l^{-1} of diuron at 48-h) the SEMs overlapped to less than and greater than 100%, respectively, suggesting minimal or no change in growth relative to the controls for most treatments (Fig. 1B). The subtle increase of growth observed at these diuron concentrations was likely due to hormesis, which is an adaptive response characterised by low-dose stimulation and high-dose inhibition (Calabrese and Baldwin, 2003). Hormesis is either directly induced, or the result of compensatory biological processes (Calabrese and Baldwin, 2002), and has been previously documented in aquatic phototrophs when exposed to sub-lethal concentrations of pesticides (Cedergreen et al., 2005, 2007).

These results suggest that diuron at concentrations of up to 3 µg l^{-1} did not stimulate nor inhibit the growth (within 20% of the controls) of *P. tricornutum* after 48- or 72-h. A poor fit of the four-parameter sigmoidal regression model to the growth inhibition data ($R^2 = \leq 0.01$ for 48 and 72-h) prevented typical stressor-response relationships from being obtained. Thus, EC_x values were not able to be accurately calculated for growth inhibition.

Previous studies reported the growth of *P. tricornutum* to be negatively affected at higher diuron concentrations and longer exposure periods than were used in the present study. For *P. tricornutum*, USEPA (2015) reported a 10-day EC_{50} (growth, biomass) value of 10 µg l^{-1} diuron while Clarkson et al. (1998) reported 3-day and 7-day EC_{50} (growth) values of 20.98 and 77 µg l^{-1} diuron, respectively. This suggests that in order to have observed inhibition of *P. tricornutum* growth after 72-h of exposure, test concentrations need to be within range of ~20 µg l^{-1} diuron. However, all diuron concentrations in this study were intentionally kept low (≤ 50% effect) to allow for increased effect (≥ 50%) when combined with reduced light availability in combined stressor tests.

3.3. Exposure to reduced light alone

3.3.1. Effects on effective quantum yield

There was a significant interaction between light and exposure duration on EQY ($\chi^2 = 76.63$, $df = 10$, $p = 2.29 \times 10^{-12}$). Relative to the controls, light alone significantly increased EQY (i.e., all treatments were > 100%; $p \leq 0.05$) of *P. tricornutum* after 72-hours of exposure at the light intensities used (Fig. 2 A). Relative to the controls, EQY was highest at the lowest light level (5 µmol photons m^{-2} s^{-1}) reaching a mean ± SEM of 157 ± 5.6% (R^2 = 0.88) at 48-hours of exposure (Fig. 2A). The EQY of the algae treatments remained ≥ 0.5 throughout the tests, whilst the controls (80 µmol photons m^{-2} s^{-1}) dropped below 0.5 (i.e., lowest of 0.3) (Supplementary material, Table S 2).

Under light limiting conditions, there is a reduction of captured photons, which ultimately leads to a reduction in electron transport (Ralph and Gademann, 2005). When this occurs, the rate of light harvesting meets the rate of electron transport, thus reducing emitted fluorescence and increasing the observed effective and maximum quantum yields of PSII (Ralph et al., 2007a). Additionally, chlorophyll content that is responsible for harvesting light will generally increase after exposure to low light levels (Zhu et al., 2017), in an attempt to

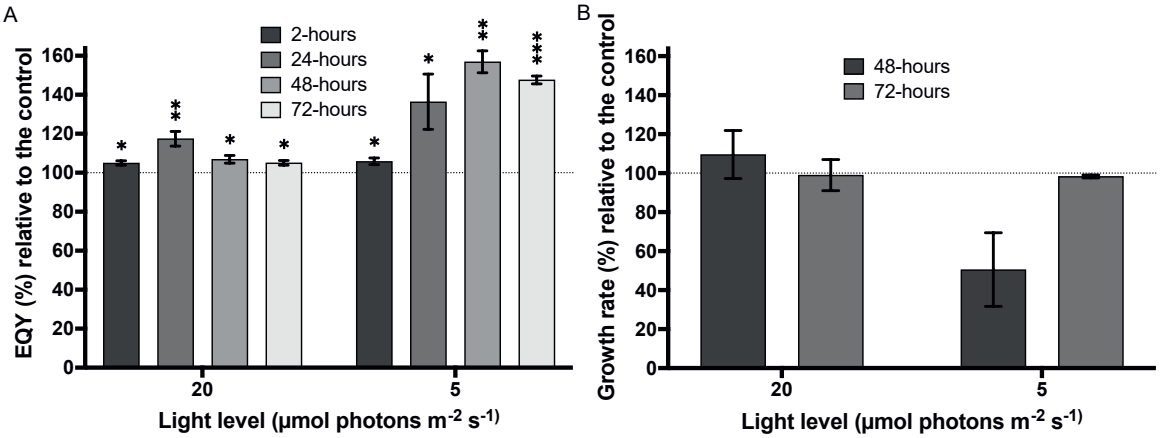

Fig. 2. Mean (± SEM) for the effective quantum yield (A; $n = 4$) and growth rate (B; $n = 3$) of *P. tricornutum* expressed as a percentage of the controls, when exposed to decreased light (from optimal). Responses (%) have been expressed as a percentage of the control (dashed line) so that the controls equal 100%, and values less than and greater than 100% indicate decreased and increased EQY/growth, respectively (e.g., 90% and 120% values on the y-axis are equivalent to 10% reduction of photosynthetic efficiency/growth and 20% increase of photosynthetic efficiency/growth relative to the controls, respectively). Asterisk (*) indicates value significantly different from the 80 µmol photons m^{-2} s^{-1} controls at each respective time point (* = $p \leq 0.05$, ** = $p \leq 0.01$, *** = $p \leq 0.001$).

compensate for any reduced photosynthetic yield (Boardman, 1977). Therefore, it is common for total chlorophyll content and quantum yield (effective and maximum) to increase within hours to days of algae being subjected to low light stress (Ralph, 1999; Ralph et al., 2007a; Dubinsky and Stambler, 2009; Li et al., 2014; Negri et al., 2015; Zhu et al., 2017). To more accurately assess the impacts of reduced light, it would be beneficial to measure pigment and chlorophyll content in addition to EQY.

3.3.2. *Effects on growth rate*

There was a significant interaction between light and exposure duration on growth rate ($\chi^2 = 17.784$, $df = 8$, $p = 0.023$). Growth was

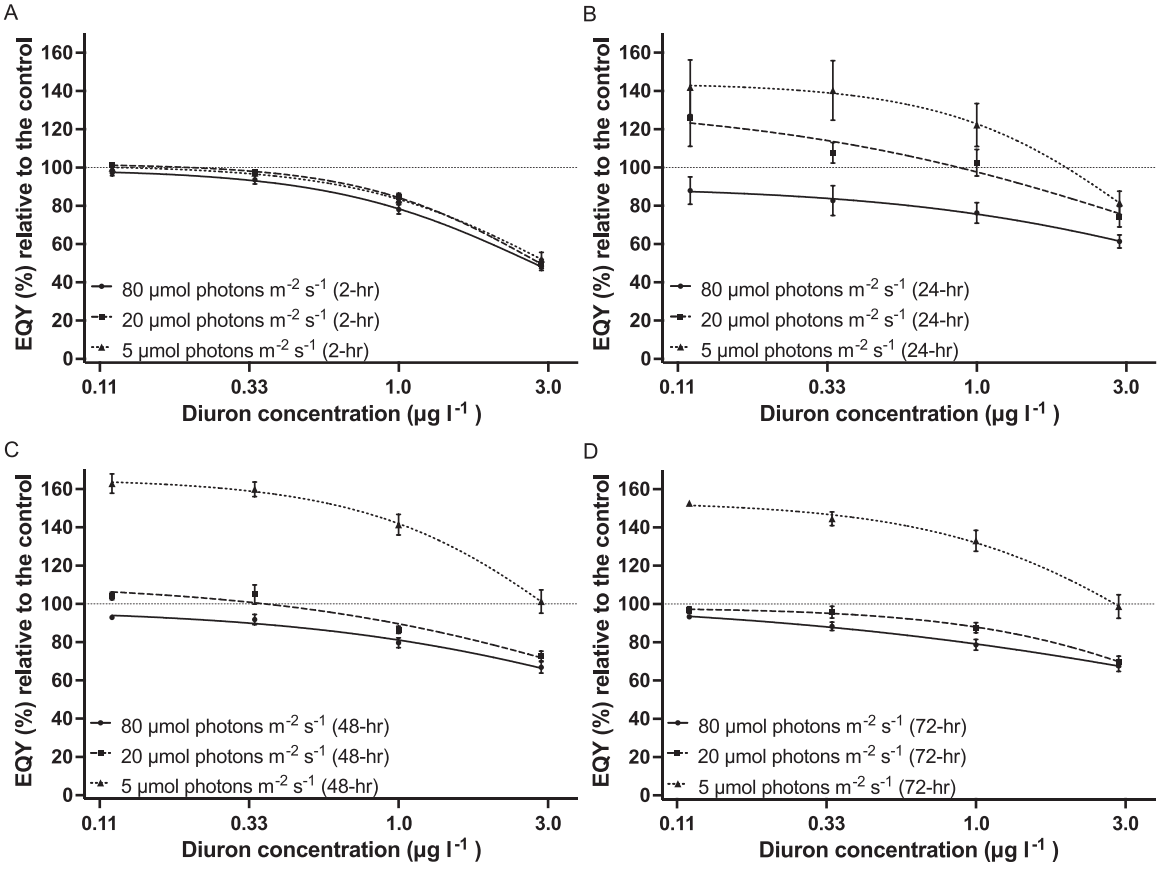

Fig. 3. Stressor response curves of the mean (± SEM) for the effective quantum yield ($n = 4$) of *P. tricornutum* expressed as a percentage of the controls, when exposed to a range of diuron concentrations at three light levels after 2-h (A), 24-h (B), 48-h (C) and 72-h (D). Responses (%) have been expressed as a percentage of the control (dashed line) so that the controls equal 100%, and values less than and greater than 100% indicate decreased and increased EQY, respectively (e.g., 90% and 120% values on the y-axis are equivalent to 10% reduction of photosynthetic efficiency and 20% increase of photosynthetic efficiency relative to the controls, respectively).

most inhibited (however not significant, $p = 0.128$) after 48-h of exposure to 5 μmol photons m^{-2} s^{-1}, with a mean ± SEM of 50 ± 19% relative to the controls. At the same low light level, the longer exposure (72-h) was very similar to the controls with a mean ± SEM of 98 ± 0.8% (Fig. 2B). Only one treatment (20 μmol photons m^{-2} s^{-1} at 48-h) slightly facilitated growth, with a mean ± SEM of 110 ± 12% (Fig. 2B).

Low-light stress may cause growth inhibition by reducing photon capture for photosynthetic processes and/or by amplifying the production of reactive oxygen species (ROS). However, chronic exposure to low light stress increases ROS-scavenging enzymes, which maintain and/or reduce ROS to normal concentrations (Barros et al., 2003; Wang et al., 2018). Thus, growth inhibition from low light stress is likely to be driven by plant starvation via reduced photosynthesis, rather than the presence of ROS (Negri et al., 2015).

3.4. Simultaneous exposure to diuron and reduced light

The simultaneous exposure of *P. tricornutum* to diuron and reduced light had less impact on EQY than diuron alone (under optimal light) at all exposure durations (2–72-h), but more of an impact on EQY than light alone at 2, 48 and 72-h (Fig. 1A, 2A and 3). For EQY, there was a significant interactive effect between diuron and all light levels ($F = 38.7$, $df = 2$, $p \leq 0.001$, $F = 86.9$, $df = 1$, $p \leq 0.001$; and, $F = 88.9$, $df = 1$, $p \leq 0.001$, for 80, 20 and 5 μmol photons m^{-2} s^{-1}, respectively). When exposed to all concentrations of diuron (0.1–3 μg l^{-1}) under the lowest light intensity (5 μmol photons m^{-2} s^{-1}), EQY typically increased with increased exposure duration (Fig. 3). For example, exposure to 3 μg l^{-1} diuron and 5 μmol photons m^{-2} s^{-1} increased EQY by 52 ± 3.5%, 82 ± 6.1%, 101 ± 6.1% and 99 ± 6.2% relative to the controls, at 2, 24, 48 and 72-hours, respectively (Fig. 3). Thus, EQY was halved after 2-hours of exposure, but then no different to the controls after 48 and 72-hours of exposure.

Effect concentration values (EC_{10} and EC_{20}) for EQY were calculated for diuron exposure under all light levels (80 – 5 μmol photons m^{-2} s^{-1}) at 2, 24, 48 and 72-h (Table 1). Typically, EC_{10} and EC_{20} (EQY) values increased with decreasing light from 80 to 5 μmol photons m^{-2} s^{-1} at each time point, suggesting that low light decreases the sensitivity of *P. tricornutum* to diuron. Trends in EC_x values with decreasing light are unlikely to be biologically meaningful at 2 and 24-h as microalgae will generally take ≤ 24-h to acclimate to low light stress before directly impacting EQY.

Growth was only significantly affected by diuron concentrations at the lowest light level (5 μmol photons m^{-2} s^{-1}) ($F = 7.769$, $df = 1$, $p = 0.006$); while, non-significant effects occurred between diuron and growth at the 80 and 20 μmol photons m^{-2} s^{-1} light levels ($F = 0.000$, $df = 1$, $p = 0.983$; and, $F = 0.099$, $df = 1$, $p = 0.753$, respectively). Relative to the controls, growth was not inhibited for any combination of diuron and the 80 or 20 μmol photons m^{-2} s^{-1} light over 72-h (Fig. 4). However, growth inhibition increased with increased diuron concentrations when simultaneously exposed to 5 μmol photons m^{-2} s^{-1}. Increasing the duration of the exposure to diuron and 5 μmol photons m^{-2} s^{-1} led to decreased growth inhibition relative to the controls.

EC_{10} and EC_{20} (growth rate) values could not be calculated at 80 (optimal) and 20 μmol photons m^{-2} s^{-1} light availability as stressor-response relationships were not observed (Table 1). As a result, best-fit values should be interpreted with caution. No EC_{10} or EC_{20} (growth rate) values were available in the literature for diuron exposure to *P. tricornutum* under optimal or reduced light availability. At the lowest light treatment (5 μmol photons m^{-2} s^{-1}), EC_x estimates were 0.30 and 0.46 μg l^{-1} at 48-h and 1.6 and 1.8 μg l^{-1} at 72-h for the EC_{10} and EC_{20} values, respectively (Table 1). To the authors knowledge, there are no studies that have reported the inhibition of growth from combined diuron exposure and low light stress on *P. tricornutum*.

3.4.1. Estimated interaction types between diuron and reduced light

The change in EQY that was observed over the 72-h exposure period (Fig. 3) is similar to the trend observed in Fig. 2, where reduced light alone had the largest increase in EQY at 48 and 72-h, and a smaller increase in EQY at 2-hours. Thus, it is evident that light reduction is having a marked effect on EQY. In order to then identify what contribution diuron is having on EQY when combined with reduced light, predicted values were calculated based on the Independent Action model (see Section 2.6) and compared to observed values (Supplementary Material, Table S 3).

For EQY, synergistic, antagonistic and response additive effects occurred for 50%, 47% and 2% of treatments, respectively (Supplementary Material, Table S 3). The strongest estimated antagonistic interactions occurred at the lower diuron concentrations (0.11–1 μg l^{-1}) under the lowest light level (5 μmol photons m^{-2} s^{-1}) at 24 and 48-h, but only in the 5 μmol photons m^{-2} s^{-1} light level at 72-h (Fig. 5A). The strongest estimated synergistic interactions occurred at the highest diuron concentration (3 μg l^{-1}) for both reduced light levels (20 and 5 μmol photons m^{-2} s^{-1}) at 2, 24, 48 and 72-h (Fig. 5A). In addition, synergies occurred for all diuron concentrations (0.1–3 μg l^{-1}) at 20 μmol photons m^{-2} s^{-1} for the 72-h exposures only (Fig. 5A).

For growth rate (Fig. 5B), estimated antagonistic interactions were

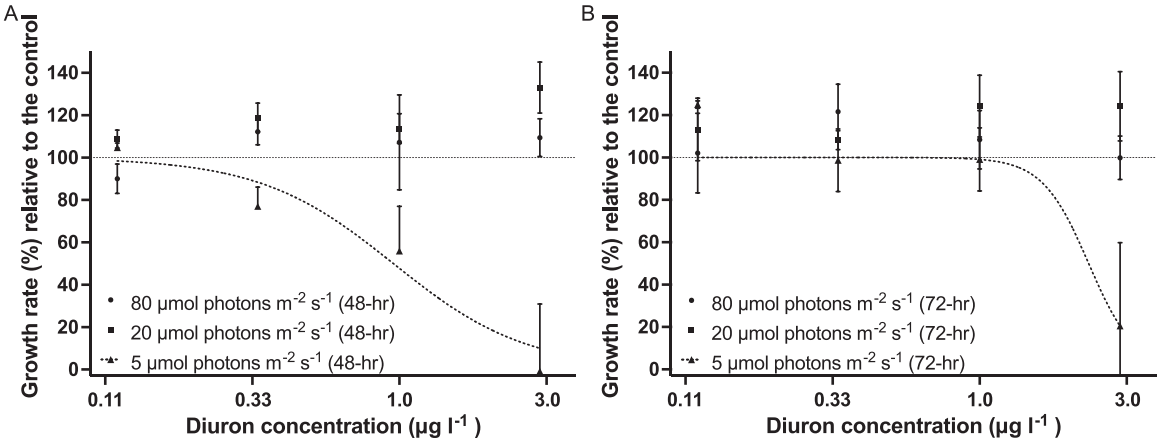

Fig. 4. Stressor response curves of the mean (± SEM) for growth rate ($n = 3$) of *P. tricornutum* expressed as a percentage of the controls, when exposed to a range of diuron concentrations at three light levels after 48-h (A) and 72-h (B). Responses (%) have been expressed as a percentage of the control (dashed line) so that the controls equal 100%, and values less than and greater than 100% indicate decreased and increased growth, respectively (e.g., 90% and 120% values on the y-axis are equivalent to 10% reduction of growth and 20% increase of growth relative to the controls, respectively). Stressor-response curves could not be fitted to the growth rate data at 80 and 20 μmol photons m^{-2} s^{-1} light level ($R^2 = < 0.5$ for 48 and 72-hours).

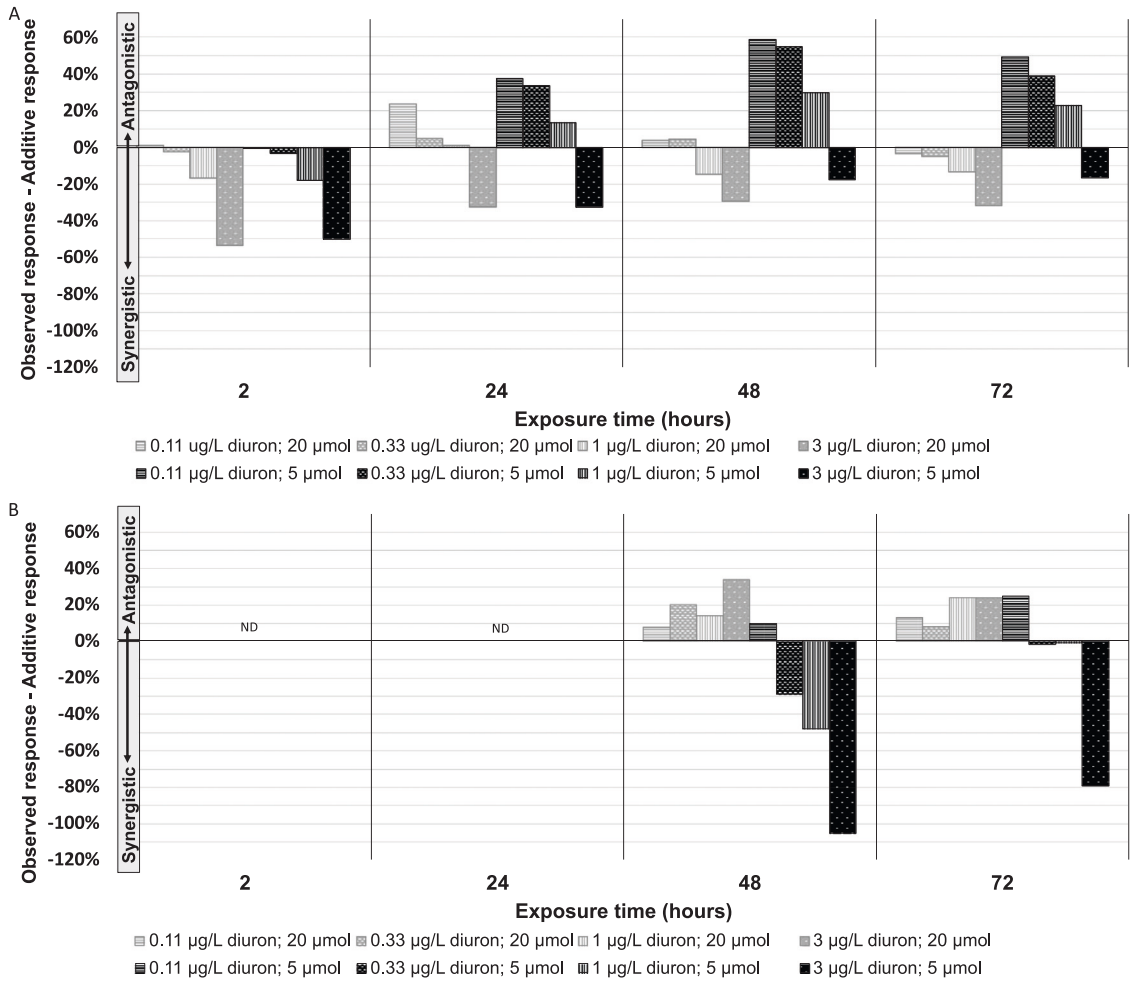

Fig. 5. Estimated types of joint action for four diuron concentrations (0.1–3 µg l^{-1}) under two reduced light scenarios of 20 µmol photons m^{-2} s^{-1} (grey) and 5 µmol photons m^{-2} s^{-1} (black) on the effective quantum yield (A) and growth rate (B) over 72-h. Positive and negative responses (%) indicate the strength of antagonistic and synergistic interactions between stressors, respectively. ND indicates no data.

more common than estimated synergistic interactions (63% and 37%, respectively). The synergies occurred only at the lowest light level (5 µmol photons m^{-2} s^{-1}) with 0.3–3 µg l^{-1} of diuron at 48 and 72-h. All other treatment combinations for growth rate were estimated to be antagonisms.

The strongest synergy for growth rate (−106%) was at 48-h when 3 µg l^{-1} diuron was combined with 5 µmol photons m^{-2} s^{-1} (Fig. 5B). Here, growth rate was most inhibited with a mean ± SEM of − 0.8 ± 32% relative to the controls (i.e., ~100% inhibition or completely inhibited) (Fig. 4). At this same time point, EQY was also synergistic (−18%) (Fig. 5A); however, this resulted in increased EQY by 1.3 ± 6.1% (which equates to 101.3% relative to the controls) (Fig. 3C).

Individually, these results suggest that EQY decreases from diuron exposure but increases from decreased light availability; while growth is relatively unaffected by the diuron concentrations used here but inhibited by low light. We surmise that in combination, the increased EQY effects from low light mitigate the decreased EQY effects from diuron, meaning that *P. tricornutum* benefits from low light conditions when exposed to diuron concentrations (Fig. 5A and B). However, there is a tipping point when exposed to 5 µmol photons m^{-2} s^{-1} of light and 3 µg l^{-1} of diuron as EQY no longer increases and growth is heavily inhibited (Fig. 5A and B).

The data suggest that exposure to a combination of diuron and low light availability heavily impacts the ability of *P. tricornutum* to harvest photons. Available photons are limited under low light conditions, limiting photosynthetic efficiency. Here, it is surmised that the higher the diuron concentration, the more plastoquinone (electron carrier) molecules will be blocked (i.e., preventing majority, or all, of photons from passing through the ETC); whereas lower diuron concentrations may allow for a portion of plastoquinone molecules to remain unblocked, which would still allow for some electron flow.

These results suggest that the greatest combined negative impact of diuron and light limitation on EQY and growth rate occurred between 48 and 72-h of exposure. However, it should be noted that the maximum exposure duration was 72-h, so the effects of longer exposures are not known. This timeframe is relevant to GBR flood plume dispersion, where diuron concentrations and suspended sediment concentrations are at their highest before dilution and dispersion with marine waters (Brodie et al., 2010; Devlin et al., 2012). Thus, the results of this study indicate that the combined impact of diuron and light limitation on phototrophs is likely to be the greatest within the first two to three days of a flood-event. Toxicity tests with longer exposure periods (e.g., 5–7 days) are required to confirm this.

3.4.2. Processes driving impact following simultaneous exposure to diuron and reduced light

Exposure of *P. tricornutum* to diuron alone reduced EQY by up to 48% relative to the controls, despite not inhibiting growth (<20%) (Fig. 1). In contrast, low light inhibited growth rate by up to 51%, but increased EQY by up to 157% relative to the controls (Fig. 2).

Following exposure to diuron, EQY responses were detected almost instantaneously at 0.3-h (data not shown) and 2-h. However, growth and

other cytotoxic responses (i.e., cell damage or mortality), which are more so cumulative measurements that reflect other underlying physiological processes, typically occurred after 12–24-h. At 24-h of simultaneous exposure of *P. tricornutum* to diuron and low light, diuron appeared to be the dominant stressor driving changes to EQY (Fig. 3A), as the different light intensities decreased EQY to similar levels. However after 24-h, it appeared that the compensatory effects of reduced light (i.e., increased EQY and/or regulated ROS concentrations) began to occur (as indicated by lower light exposures), leading to increased EQY (i.e., greater photosynthetic efficiency) at these longer exposure periods (Fig. 3B, C, D).

In contrast, low light intensity was the dominant stressor driving stimulation of growth rate (Fig. 4), as diuron concentrations were too low to trigger growth inhibition over the 72-hour exposure period (Fig. 1B). High variability in growth rate data was observed at 24-h (data not shown); however, clear trends of growth inhibition were observed at 48 and 72-h when *P. tricornutum* was simultaneously exposed to diuron and reduced light (Fig. 4). At 48-hours, reduced light alone caused a maximum growth inhibition value of 51 ± 19% (mean ± SEM) relative to the controls (Fig. 2A); though when paired with the highest tested diuron concentration of 3 μg l^{-1}, growth rate dropped further to − 1 ± 32% relative to the controls, which equates to a total of 101 ± 32% growth inhibition (Fig. 4B). Interestingly, at 72-hours reduced light alone did not affect growth rate (98 ± 0.8%) relative to the controls, until paired with 3 μg l^{-1} of diuron, where growth rate decreased to 20 ± 39% (mean ± SEM) relative to the controls (Fig. 4). As a result, the combined effects on EQY and growth rate were exacerbated when *P. tricornutum* was simultaneously exposed to high diuron (≥ 3 μg l^{-1}) and low light availability (5 μmol photons m^{-2} s^{-1}).

These findings suggest that multiple physiological responses in marine diatoms can be simultaneously impacted by PSII-inhibiting herbicides and low light. For example, low light increases chlorophyll content (aiding photosynthesis and growth) (Boardman, 1977), whilst diuron simultaneously reduces photosynthetic efficiency (via decreased EQY), but increases intracellular ROS concentrations and hence, hinders growth (Ahrens, 1994; King et al., 2021). These results highlight the importance of measuring; multiple physiological responses across different levels of biological organisation (i.e., physiological and whole-organism effects), and, both acute and chronic exposure durations (i.e., up to and greater than 3-days) (George et al., 2014; Ferreira et al., 2016) to accurately quantify the combined impacts of diuron and reduced light on photosynthetic organisms.

Although pesticide concentrations can be relatively high in some freshwater catchments, these concentrations become increasingly dilute as river waters mix with inshore marine waters (Lewis et al., 2009). In the most recent pesticide monitoring data for the inshore portion of the GBR lagoon, diuron was the most frequently detected PSII-inhibiting herbicide (detected in 88% of passive samplers in 2017–18 and > 90% in 2018–19), closely followed by atrazine and hexazinone (Gallen et al., 2019; Thai et al., 2020). The maximum detected concentrations of diuron in the GBR lagoon were 0.8 and 0.3 μg l^{-1} in 2017–18 and 2018–19, respectively (Gallen et al., 2019; Thai et al., 2020), which fall within the range of diuron concentrations used for exposure tests in the present study (0.1–3 μg l^{-1}). In Australia, the proposed default guideline value (ecosystem protection) to protect 99% of marine species from harmful effects of diuron is 0.43 μg l^{-1} (King et al., 2017). The 99% protection value is recommended for use in high conservation value systems such as the GBR (Warne et al., 2018). The measured maximum environmental concentrations of 0.3 and 0.8 μg l^{-1} of diuron (Gallen et al., 2019; Thai et al., 2020) correspond to affecting < 1 to ~10% of marine species. Thus, posing a very low to moderate risk to aquatic organisms (Warne et al., 2020a). The present study highlighted that the overall risk (from combined EQY and growth rate effects) of these environmentally relevant diuron concentrations may be worsened under reduced light availability (Fig. 4). Despite inshore PSII-inhibiting herbicide concentrations generally being low (Gallen et al., 2019; Thai et al., 2020), it is important to understand their combined and/or interactive effects with other pesticides (Spilsbury et al., 2020; Warne et al., 2020b), as well as non-chemical stressors such as light (Sjollema et al., 2014b), nutrients and sediments (Waterhouse et al., 2017), elevated sea surface temperature (Negri et al., 2020) and ocean acidification (Flores et al., 2021). In doing so, more rigorous and realistic ecotoxicological risk characterisations can be developed for the implementation of environmental management.

4. Conclusions

This study found that reduced light negatively affects the phytotoxicity of diuron to the diatom, *P. tricornutum*. In addition, it highlights; 1) the importance of measuring effects after various exposure periods to identify when physiological responses occur over time; and, 2) the importance of measuring endpoints across different levels of biological organisation (i.e., physiological and whole-organism). Measuring various endpoints can reflect the numerous modes of action being impacted by the specific stressors. In doing so, a more accurate representation of the combined net effects can be quantified. These results indicate that reducing suspended sediment and diuron concentrations in marine waters can decrease harmful effects on *P. tricornutum*. It is plausible that these findings would apply to other PSII-inhibiting herbicides, other diatoms and potentially to other photosynthetic organisms.

Funding

Olivia C. King was supported by an Australian Government Research Training Program Stipend Scholarship; Christopher J. Brown was supported by a Discovery Project grant (DP180103124) from the Australian Research Council.

CRedit author statement

OK carried out the conceptualization, laboratory work, data curation, statistical analyses and wrote the manuscript. JvM participated in methodology development, study design, laboratory investigation and revised the manuscript. MW and CB assisted with early conceptualization, formal analyses and drafts as well as critical revisions of the manuscript. CB also assisted with funding acquisition. RS supervised study conceptualization, laboratory investigation, data and formal analyses, drafts and critical revisions of the manuscript. All authors gave the final approval for publication and agree to be held accountable for the work performed therein.

Declaration of Competing Interest

The authors declare that they have no known competing financial interests or personal relationships that could have appeared to influence the work reported in this paper.

Appendix A. Supporting information

Supplementary data associated with this article can be found in the online version at doi:10.1016/j.ecoenv.2022.113729.

References

Ahrens, W.H., 1994. Herbicide Handbook of the Weed Science Society of America. Weed Science Society of America, Champaign, Illinois, United States of America.
Armbrust, E.V., 2009. The life of diatoms in the world's oceans. Nature 459, 185–192.
Arrigo, K.R., 2005. Marine microorganisms and global nutrient cycles. Nature 437, 349–355.
Australian Government and Queensland Governments, 2018. Reef 2050 Water Quality Improvement Plan 2017 – 2022. Reef Water Quality Protection Plan Secretariat, Queensland, Australia.

Barros, M.P., Pedersen, M., Colepicolo, P., Snoeijs, P., 2003. Self-shading protects phytoplankton communities against H2O2-induced oxidative damage. Aquat. Microb. Ecol. 30, 275–282.
BCPC, 2012. The Pesticide Manual. British Crop Production Council (BCPC), Alton, United Kingdom.
Bell, P.R., Elmetri, I., 1995. Ecological indicators of large-scale eutrophication in the Great Barrier Reef lagoon. Oceanogr. Lit. Rev. 12, 1145.
Bengtson Nash, S.M., Quayle, P.A., Schreiber, U., Müller, J.F., 2005. The selection of a model microalgal species as biomaterial for a novel aquatic phytotoxicity assay. Aquat. Toxicol. 72, 315–326.
Bliss, C.I., 1939. The toxicity of poisons applied jointly. Ann. Appl. Biol. 26, 585–615.
Boardman, N.K., 1977. Comparative photosynthesis of sun and shade plants. Annu. Rev. Plant Physiol. 28, 355–377.
Brodie, J., Schroeder, T., Rohde, K., Faithful, J., Masters, B., Dekker, A., Brando, V., Maughan, M., 2010. Dispersal of suspended sediments and nutrients in the Great Barrier Reef lagoon during river-discharge events: conclusions from satellite remote sensing and concurrent flood-plume sampling. Mar. Freshw. Res. 61, 651–664.
Brodie, J., Waterhouse, J., Schaeffer, B., Furnas, M., Maynard, J.A., Collier, C., Lewis, S., Warne, M., Fabricus, K., Devlin, M., McKenzie, L., Yorkston, H., Randall, L., Bennett, J., Brando, V., 2013. Chapter 3: Relative risks to the Great Barrier Reef from degraded water quality. Scientific Consensus Statement 2013: Land Use Impacts on Great Barrier Reef Water Quality and Ecosystem Condition. Reef Water Quality Protection Plan Secretariat, Brisbane.
Brown, C.J., Saunders, M.I., Possingham, H.P., Richardson, A.J., 2014. Interactions between global and local stressors of ecosystems determine management effectiveness in cumulative impact mapping. Divers. Distrib. 20, 538–546.
Calabrese, E.J., Baldwin, L.A., 2002. Defining hormesis. Hum. Exp. Toxicol. 21, 91–97.
Calabrese, E.J., Baldwin, L.A., 2003. Hormesis: the dose-response revolution. Annu. Rev. Pharmacol. Toxicol. 43, 175–197.
Cedergreen, N., Ritz, C., Streibig, J.C., 2005. Improved empirical models describing hormesis. Environ. Toxicol. Chem. Int. J. 24, 3166–3172.
Cedergreen, N., Streibig, J.C., Kudsk, P., Mathiassen, S.K., Duke, S.O., 2007. The occurrence of hormesis in plants and algae. Dose-Response 5 dose-response.06-008. Cedergreen.
Chariton, A.A., Sun, M., Gibson, J., Webb, J.A., Leung, K.M.Y., Hickey, C.W., Hose, G.C., 2016. Emergent technologies and analytical approaches for understanding the effects of multiple stressors in aquatic environments. Mar. Freshw. Res. 67, 414–428.
Chen, S., Yin, C., Strasser, R.J., GovindjeeYang, C., Qiang, S., 2012. Reactive oxygen species from chloroplasts contribute to 3-acetyl-5-isopropyltetramic acid-induced leaf necrosis of *Arabidopsis thaliana*. Plant Physiol. Biochem. 52, 38–51.
Clarkson, N., Leftley, J.W., Meldrum, D.T., Watson, J.W., 1998. An assessment of the cage-culture turbidostat as an alternative algal bioassay. Water Res. 32, 1162–1168.
Côté, I.M., Darling, E.S., Brown, C.J., 2016. Interactions among ecosystem stressors and their importance in conservation. Proc. R. Soc. Ser. B Biol. Sci. 283, 1–9.
Crain, C.M., Kroeker, K., Halpern, B.S., 2008. Interactive and cumulative effects of multiple human stressors in marine systems. Ecol. Lett. 11, 1304–1315.
Devlin, M.J., McKinna, L.W., Álvarez-Romero, J.G., Petus, C., Abott, B., Harkness, P., Brodie, J., 2012. Mapping the pollutants in surface riverine flood plume waters in the Great Barrier Reef, Australia. Mar. Pollut. Bull. 65, 224–235.
Du, G.-y, Zhong, X.-f, Dupuy, C., Che, S., Lavaud, J., 2021. Diuron effects on photosynthesis and vertical migration of microphytobenthos: potential rapid bioassessment of herbicide toxicity in coastal sediments. Mar. Pollut. Bull. 170, 112619.
Dubinsky, Z., Stambler, N., 2009. Photoacclimation processes in phytoplankton: mechanisms, consequences, and applications. Aquat. Microb. Ecol. 56, 163–176.
Escher, B., Bramaz, N., Mueller, J., Quayle, P., Rutishauser, S., Vermeirssen, E., 2008. Toxic equivalent concentrations (TEQs) for baseline toxicity and specific modes of action as a tool to improve interpretation of ecotoxicity testing of environmental samples. J. Environ. Monit. 10, 612–621.
Fabricius, K.E., Logan, M., Weeks, S., Brodie, J., 2014. The effects of river run-off on water clarity across the central Great Barrier Reef. Mar. Pollut. Bull. 84, 191–200.
Ferreira, V., Pinto, R., Sant'Anna, C., 2016. Low light intensity and nitrogen starvation modulate the chlorophyll content of *Scenedesmus dimorphus*. J. Appl. Microbiol. 120, 661–670.
Flores, F., Marques, J.A., Uthicke, S., Fisher, R., Patel, F., Kaserzon, S., Negri, A.P., 2021. Combined effects of climate change and the herbicide diuron on the coral *Acropora millepora*. Mar. Pollut. Bull. 169, 112582.
Gallen, C., Thai, P., Paxman, C., Prasad, P., Elisei, G., Reeks, T., Eaglesham, G., Yeh, R., Tracey, D., Grant, S., 2019. Marine Monitoring Program: Annual Report for Inshore Pesticide Monitoring 2017-18. Great Barrier Reef Marine Park Authority, Townsville.
George, B., Pancha, I., Desai, C., Chokshi, K., Paliwal, C., Ghosh, T., Mishra, S., 2014. Effects of different media composition, light intensity and photoperiod on morphology and physiology of freshwater microalgae *Ankistrodesmus falcatus* – A potential strain for bio-fuel production. Bioresour. Technol. 171, 367–374.
Gomes, M.P., Juneau, P., 2017. Temperature and light modulation of herbicide toxicity on algal and cyanobacterial physiology. Front. Environ. Sci. 5.
Howe, P.L., Reichelt-Brushett, A.J., Clark, M.W., Seery, C.R., 2017. Toxicity estimates for diuron and atrazine for the tropical marine cnidarian *Exaiptasia pallida* and in-hospite *Symbiodinium* spp. using PAM chlorophyll-a fluorometry. J. Photochem. Photobiol. B Biol. 171, 125–132.
ISO, 2016. Water quality - Marine Algal Growth Inhibition Test with *Skeletonema sp.* and *Phaeodactylum tricornutum*. International Organisation for Standardisation (ISO), Switzerland. ISO: 10253:2016.
King, O., Smith, R., Mann, R., Warne, S.J.M., 2017. Proposed Aquatic Ecosystem Protection Guideline Values for Pesticides Commonly Used in the Great Barrier Reef catchment area: Part 1 (amended) - 2,4-D, Ametryn, Diuron, Glyphosate, Hexazinone, Imazapic, Imidacloprid, Isoxaflutole, Metolachlor, Metribuzin, Metsulfuron-methyl, Simazine, Tebuthiuron. Department of Environment and Science, Brisbane, Queensland, Australia.
King, O.C., Smith, R.A., Warne, M.St.J., van de Merwe, J.P., Connolly, R.M., Brown, C.J., 2021. Combined impacts of photosystem II-inhibiting herbicides and light availability on seagrass and marine microalgae. Mar. Ecol. Prog. Ser. 668, 215–230.
Kreyling, J., Schweiger, A.H., Bahn, M., Ineson, P., Migliavacca, M., Morel-Journel, T., Christiansen, J.R., Schtickzelle, N., Larsen, K.S., 2018. To replicate, or not to replicate – that is the question: how to tackle nonlinear responses in ecological experiments. Ecol. Lett. 21, 1629–1638.
Lee, K.-S., Park, S.R., Kim, Y.K., 2007. Effects of irradiance, temperature, and nutrients on growth dynamics of seagrasses: a review. J. Exp. Mar. Biol. Ecol. 350, 144–175.
Lewis, S.E., Brodie, J.E., Bainbridge, Z.T., Rohde, K.W., Davis, A.M., Masters, B.L., Maughan, M., Devlin, M.J., Mueller, J.F., Schaffelke, B., 2009. Herbicides: a new threat to the Great Barrier Reef. Environ. Pollut. 157, 2470–2484.
Li, Y., Xu, J., Gao, K., 2014. Light-modulated responses of growth and photosynthetic performance to ocean acidification in the model diatom *Phaeodactylum tricornutum*. PLoS One 9, e96173.
Magnusson, M., Heimann, K., Negri, A.P., 2008. Comparative effects of herbicides on photosynthesis and growth of tropical estuarine microalgae. Mar. Pollut. Bull. 56, 1545–1552.
Magnusson, M., Heimann, K., Quayle, P., Negri, A.P., 2010. Additive toxicity of herbicide mixtures and comparative sensitivity of tropical benthic microalgae. Mar. Pollut. Bull. 60, 1978–1987.
Marzonie, M., Flores, F., Sadoun, N., Thomas, M.C., Valada-Mennuni, A., Kaserzon, S., Mueller, J.F., Negri, A.P., 2021. Toxicity thresholds of nine herbicides to coral symbionts (Symbiodiniaceae). Sci. Rep. 11, 21636.
Maxwell, K., Johnson, G.N., 2000. Chlorophyll fluorescence—a practical guide. J. Exp. Bot. 51, 659–668.
Morin, S., Chaumet, B., Mazzella, N., 2018. A time-dose response model to assess diuron-induced photosynthesis inhibition in freshwater biofilms. Front. Environ. Sci. 6.
Muller, R., Schreiber, U., Escher, B.I., Quayle, P., Nash, S.M.B., Mueller, J.F., 2008. Rapid exposure assessment of PSII herbicides in surface water using a novel chlorophyll a fluorescence imaging assay. Sci. Total Environ. 401, 51–59.
Negri, A.P., Flores, F., Mercurio, P., Mueller, J.F., Collier, C.J., 2015. Lethal and sub-lethal chronic effects of the herbicide diuron on seagrass. Aquat. Toxicol. 165, 73–83.
Negri, A.P., Smith, R.A., King, O., Frangos, J., Warne, M.S.J., Uthicke, S., 2020. Adjusting tropical marine water quality guideline values for elevated ocean temperatures. Environ. Sci. Technol. 54, 1102–1110.
OECD, 2011. Test No. 201: Freshwater Alga and Cyanobacteria, Growth Inhibition Test. Organisation for Economic Co-operation and Development (OECD) Publishing, Paris, France.
Ralph, P.J., 1999. Light-induced photoinhibitory stress reponses of laboratory-cultured *Halophila ovalis*. Bot. Mar. 42, 11–22.
Ralph, P.J., Durako, M.J., Enríquez, S., Collier, C.J., Doblin, M.A., 2007a. Impact of light limitation on seagrasses. J. Exp. Mar. Biol. Ecol. 350, 176–193.
Ralph, P.J., Gademann, R., 2005. Rapid light curves: a powerful tool to assess photosynthetic activity. Aquat. Bot. 82, 222–237.
Ralph, P.J., Smith, R.A., Macinnis-Ng, C.M.O., Seery, C.R., 2007b. Use of fluorescence-based ecotoxicological bioassays in monitoring toxicants and pollution in aquatic systems: review. Toxicol. Environ. Chem. 89, 589–607.
Reynolds, P.L., Richardson, J.P., Duffy, J.E., 2014. Field experimental evidence that grazers mediate transition between microalgal and seagrass dominance. Limnol. Oceanogr. 59, 1053–1064.
Riedl, J., Altenburger, R., 2007. Physicochemical substance properties as indicators for unreliable exposure in microplate-based bioassays. Chemosphere 67, 2210–2220.
Schreiber, U., Müller, J.F., Haugg, A., Gademann, R., 2002. New type of dual-channel PAM chlorophyll fluorometer for highly sensitive water toxicity biotests. Photosynth. Res. 74, 317–330.
Schreiber, U., Quayle, P., Schmidt, S., Escher, B.I., Mueller, J.F., 2007. Methodology and evaluation of a highly sensitive algae toxicity test based on multiwell chlorophyll fluorescence imaging. Biosens. Bioelectron. 22, 2554–2563.
Sjollema, S.B., MartínezGarcía, G., van der Geest, H.G., Kraak, M.H.S., Booij, P., Vethaak, A.D., Admiraal, W., 2014a. Hazard and risk of herbicides for marine microalgae. Environ. Pollut. 187, 106–111.
Sjollema, S.B., Vavourakis, C.D., van der Geest, H.G., Vethaak, A.D., Admiraal, W., 2014b. Seasonal variability in irradiance affects herbicide toxicity to the marine flagellate *Dunaliella tertiolecta*. Front. Mar. Sci. 1, 1–5.
Smale, D.A., Wernberg, T., Oliver, E.C.J., Thomsen, M., Harvey, B.P., Straub, S.C., Burrows, M.T., Alexander, L.V., Benthuysen, J.A., Donat, M.G., Feng, M., Hobday, A. J., Holbrook, N.J., Perkins-Kirkpatrick, S.E., Scannell, H.A., Sen Gupta, A., Payne, B. L., Moore, P.J., 2019. Marine heatwaves threaten global biodiversity and the provision of ecosystem services. Nat. Clim. Change 9, 306–312.
Spilsbury, F.D., Warne, M.S.J., Backhaus, T., 2020. Risk assessment of pesticide mixtures in Australian rivers discharging to the Great Barrier Reef. Environ. Sci. Technol. 54, 14361–14371.
Thai, P., Paxman, C., Prasad, P., Elisei, G., Reeks, T., Eaglesham, G., Yeh, R., Tracey, D., Grant, S., Mueller, J., 2020. Marine Monitoring Program: Annual Report for Inshore Pesticide Monitoring 2018–19. Great Barrier Reef Marine Park Authority, Townsville.
Thomas, M.C., Flores, F., Kaserzon, S., Reeks, T.A., Negri, A.P., 2020. Toxicity of the herbicides diuron, propazine, tebuthiuron, and haloxyfop to the diatom *Chaetoceros muelleri*. Sci. Rep. 10, 19592.

USEPA, 2012. OCSPP 850.4500: algal toxicity. Ecological Effects Test Guidelines. Office of Chemical Safety and Pollution Prevention: United States Environmental Protection Agency (USEPA).

USEPA, 2015. Office of Pesticide Programs Database. United States Environmental Protection Agency, Office of Prevention, Pesticides, and Toxic Substances, Washington, D.C.

Van den Brink, P.J., Choung, C.B., Landis, W., Mayer-Pinto, M., Pettigrove, V., Scanes, P., Smith, R., Stauber, J., 2016. New approaches to the ecological risk assessment of multiple stressors. Mar. Freshw. Res. 67, 429–439.

Wang, L., Zhang, X., Chen, W., Xiao, T., Zhao, X., Ma, Y., Huang, X., 2018. Shading reduced the injury caused by winter chill on Pitaya plant. Not. Bot. Horti Agrobot. Cluj. -Napoca 47, 470.

Warne, M.S.J., Batley, G., van Dam, R., Chapman, J., Fox, D., Hickey, C. & Stauber, J. 2018. Revised method for deriving Australian and New Zealand water quality guideline values for toxicants – update of 2015 version. Information Technology and Innovation, Brisbane, Queensland. Prepared for the revision of the Australian and New Zealand Guidelines for Fresh and Marine Water Quality. Australian and New Zealand Governments and Australian State and Territory Governments, Canberra.

Warne, M.S.J., Neelamraju, C., Strauss, J., Smith, R., Turner, R., Mann, R., 2020a. Development of a Method for Estimating the Toxicity of Pesticide Mixtures and a Pesticide Risk Baseline for the Reef 2050 Water Quality Improvement Plan. Department of Environment and Science, Queensland Government, Brisbane.

Warne, M.S.J., Smith, R.A., Turner, R.D.R., 2020b. Analysis of pesticide mixtures discharged to the lagoon of the Great Barrier Reef, Australia. Environ. Pollut. 265, 114088.

Waterhouse, J., Brodie, J., Tracey, D., Smith, R., Vandergragt, M., Collier, C., Petus, C., Baird, M., Kroon, F., Mann, R., Sutcliffe, T., Waters, D., Adame, F., 2017. Chapter 3: The risk from anthropogenic pollutants to Great Barrier Reef coastal and marine ecosystems. Scientific Consensus Statement 2017: A Synthesis of the Science of Land-based Water Quality Impacts on the Great Barrier Reef. Reef Water Quality Protection Plan Secretariat, Brisbane, Australia.

Waterhouse, J., Gruber, R., Logan, M., Petus, C., Howley, C., Lewis, S., Tracey, D., James, C., Mellors, J. & Tonin, H. 2021. Marine Monitoring Program: Annual report for inshore water quality monitoring 2019–20.

Zhu, H., Li, X., Zhai, W., Liu, Y., Gao, Q., Liu, J., Ren, L., Chen, H., Zhu, Y., 2017. Effects of low light on photosynthetic properties, antioxidant enzyme activity, and anthocyanin accumulation in purple pak-choi (*Brassica campestris* ssp. Chinensis Makino). PLoS One 12 e0179305-e0179305.